JOURNAL OF MORPHOLOGY 273:586–595 (2012)

New Perspectives on Collagen Fibers in the Squid Mantle

Michael Krieg[1,3] and Kamran Mohseni*[1,2,3]

[1]*Mechanical and Aerospace Engineering Department, Gainesville, Florida*
[2]*Electrical and Computer Engineering Department, Gainesville, Florida*
[3]*Institute for Cyber Autonomous Systems, University of Florida, Gainesville, Florida*†

ABSTRACT The squid mantle is a complex structure which, in conjunction with a highly sensitive sensory system, provides squid with a wide variety of highly controlled movements. This article presents a model describing systems of collagen fibers that give the mantle its shape and mechanical properties. The validity of the model is verified by comparing predicted optimal fiber angles to actual fiber angles seen in squid mantle. The model predicts optimal configurations for multiple fiber systems. It is found that the tunic fibers (outer collagen layers) provide optimal jetting characteristics when oriented at 31°, which matches empirical data from previous studies. The model also predicted that a set of intramuscular fibers (IM-1) are oriented relative to the longitudinal axis to provide optimal energy storage capacity within the limiting physical bounds of the collagen fibers themselves. In addition, reasons for deviations from the predicted values are analyzed. This study illustrates how the squid's reinforcing collagen fibers are aligned to provide several locomotory advantages and demonstrates how this complex biological process can be accurately modeled with several simplifying assumptions. J. Morphol. 273:586–595, 2012. © 2012 Wiley Periodicals, Inc.

KEY WORDS: squid mantle; collagen fibers; structure; energy storage capacity; optimization

INTRODUCTION

Squid jet propulsion produces the fastest swimming velocities seen in aquatic invertebrates (O'Dor and Webber, 1991; Anderson and Grosenbaugh, 2005). Although jetting is an inherently less efficient form of locomotion than undulatory swimming (O'Dor and Webber, 1991; Vogel, 2003), squid morphology has evolved to fully exploit it. Soaring and climbing vertically through ocean currents, negotiating prey capture, or hovering near the surface are a few of the squid's many swimming capabilities (O'Dor and Webber, 1991). The fluid dynamics of propulsive jetting in squid, and other jetting invertebrates such as jellyfish has inspired a great deal of research (Dabiri et al., 2006; Lipinski and Mohseni, 2009; Sahin and Mohseni, 2009; Sahin et al., 2009). However, the physiology of the squid mantle structure, which plays an integral part in creating the propulsive jet, has received less attention.

In general, jetting locomotion begins when the squid inhales seawater through a pair of vents or aperture behind the head, filling the mantle cavity. The mantle then contracts forcing fluid out through the funnel which rolls into a high momentum vortex ring and imparts the necessary propulsive force (Anderson and Grosenbaugh, 2005). The versatility of the system permits both low-speed steady swimming or cruising, and fast impulsive escape jetting. Two distinct gaits are seen in steady swimming as determined by the nature of the expelled jet (Bartol et al., 2009) (those being above or below the jet formation number). During cruising, squid swim at nominal speed with a higher efficiency; whereas, escape jetting involves a hyperinflation of the mantle followed by a fast powerful contraction to impart significant acceleration at the cost of fluid dynamic losses; similar to the loss in efficiency seen in high velocity jet locomotion of jellyfish (Sahin et al., 2009).

The squid mantle has a complex collagen fiber system that provides structural support and stores elastic potential energy to reduce reliance on muscle force during both the inhalant and exhalant phases (Ward and Wainwright, 1972; Gosline and Shadwick, 1983; Thompson and Kier, 2001a). This study develops a mathematical model to predict the effect that structural dynamics related to fiber orientation have on both jetting thrust (which we relate to volume constraints) and potential energy storage capacity of the mantle. Although the model is rather simplistic (treating the mantle as a

Contract grant sponsor: Office of Naval Research; Contract grant number: 1545312.

†Some initial testing was performed at the University of Colorado, Boulder.

Kamran Mohseni, University of Florida, PO Box 116250, Gainesville, FL 32611. E-mail: mohseni@ufl.edu

Received 30 June 2011; Revised 19 September 2011; Accepted 9 October 2011

Published online 18 January 2012 in Wiley Online Library (wileyonlinelibrary.com)
DOI: 10.1002/jmor.20003

© 2012 WILEY PERIODICALS, INC.

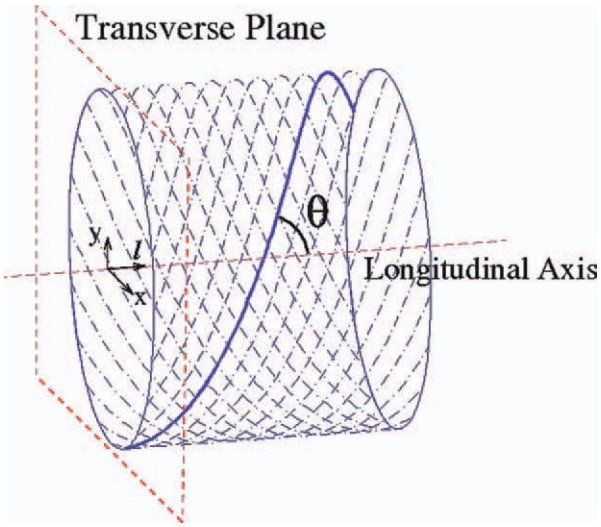

Fig. 1. The squid tunic fibers are wound in a spiral helix arrangement, and are oriented at a uniform angle (θ) to the longitudinal axis. The tunic fibers form a cylindrical tube with length L and radius a. Although the tunic consists of multiple layers of spiraling fibers only a single layer is shown for clarity. [Color figure can be viewed in the online issue, which is available at wileyonlinelibrary.com.]

straight uniform cylinder, despite the tapered shape of actual squid mantle), it takes key features of the structural dynamics into account which have largely gone ignored in previous models; such as the nonuniform strain distribution in mantle thickness and nonzero deformation in the longitudinal direction. Although these issues might seem trivial in such a simplified model, they actually allow for an optimal arrangement to be determined which helps to explain the regular layout of collagen fibers seen in the squid mantle. This analysis provides new insight to the function of the fibers.

The Squid Mantle

The powerful squid mantle primarily consists of muscle packed between two helically wound collagenous tunics which are oriented at an angle of $\sim 27^\circ \pm 1^\circ$ to the longitudinal axis of the squid, for *Lolliguncula brevis* (Ward and Wainwright, 1972). The arrangement of a single layer of collagen fibers in the tunic and a definition of the tunic fiber angle, θ, are shown in Figure 1. Circumferential muscles ring the mantle and radial muscles run from the inner tunic to the outer tunic (Fig. 2). The robust nature of the collagen fibers in the tunic, their inelastic properties, and low axial angle suggest that they act to prevent elongation and deformation of the mantle tissue during jetting.

Wound through the muscle layer, are three systems of intramuscular (IM) collagen fibers conventionally dubbed, IM-1, IM-2, and IM-3. IM-1 runs at an oblique angle through the muscle layer that is difficult to measure unless the angle is known *a priori*. Measurements of the IM-1 fiber angle relative to the squid's long axis, therefore, rely on both sagittal and tangential sections (see Fig. 2 for definition of primary sections) to accurately describe the path. We will refer to the respective fiber angles in these planes (demarcated by some authors as IM-1 sag and IM-1 tan) as β and λ. Values differing by as much as 20° are reported for both β and λ. Ward and Wainright (1972) measured β in *L. brevis* at 28°. Bone et al. (1981) measured λ at 15° in *Alloteuthis subulata*. MacGillivray et al. (1999) reported similar values in *Loligo pealei*. These low angles are in contrast to those reported by Thompson and Kier (2001a), who measured an angle of 43° for β and 32° for λ in juvenile *Sepioteuthis lessoniana* (although this value varies significantly throughout ontogeny). Thompson and Kier (2001a) suggest that the less streamlined appearance of hatchling and juvenile squid is related to the larger fiber angles. The differences between findings may also have resulted from species differences, or largely different ratio of mantle cavity volume to total volume as will be discussed in sections Maximizing Energy Storage and Results.

The exhalant phase of the jetting cycle begins when the squid contracts the circumferential muscles reducing the circumference of the mantle and thickening the muscle layer, while producing

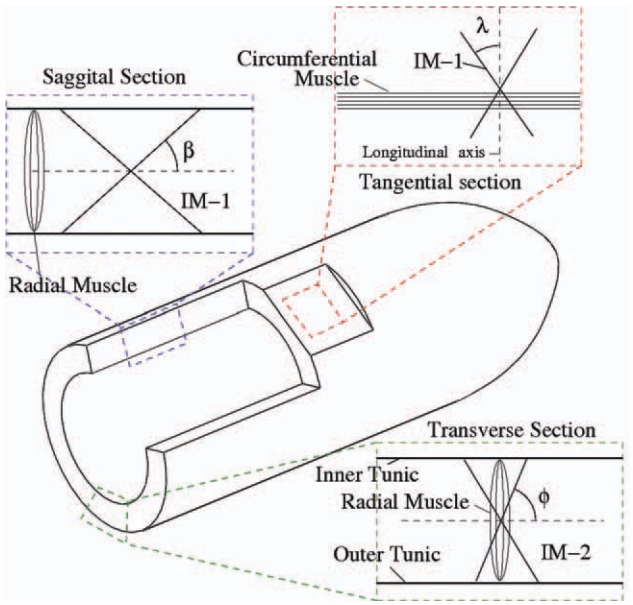

Fig. 2. Conceptual diagram of the squid mantle structure. Depicted are the three primary reference planes defining the (IM) collagen fiber angles, and the muscle structure. The sagittal plane cuts through and runs parallel to the longitudinal axis; the tangential plane runs parallel to the longitudinal axis and is locally tangent to the surface; the transverse plane runs normal to the longitudinal axis. IM-1 fibers run at oblique angles through the mantle and form angles β and λ with the longitudinal axis in the sagittal and tangential sections, respectively. The IM-2 fibers are found localized in the radial muscles and form an angle φ with the circumferential axis in the transverse plane. [Color figure can be viewed in the online issue, which is available at wileyonlinelibrary.com.]

only a small increase in length (Trueman and Packard, 1968; Ward and Wainwright, 1972). The rapid reduction in the mantle cavity volume forces seawater through the funnel and results in a high-energy jet that rapidly accelerates the squid. After coasting, the inhalant phase begins and the inner and outer tunics are brought closer together, thinning the muscle layer (Young, 1938). This is achieved by a combination of radial muscle contraction and energy transfer from deformed IM-1 and IM-2 fibers (Gosline and Shadwick, 1983). In fact, it was shown that the refilling of the mantle cavity can occur in the absence of any radial muscle power (Gosline et al., 1983).

Regardless of the measurement discrepancies, the function of the IM-1 fibers is generally agreed on. During the circumferential muscle contraction, the muscle layer thickens, and as the collagen fibers are stretched they store elastic potential energy. Once the circumferential muscles relax, the fibers pull the tunics closer together and increase the mantle circumference. We will show that the orientation of these fibers allows them to store an optimal amount of energy during contraction in the Results Section.

The IM-2 measurements have been more consistent between studies. When mantle tissue was viewed in transverse sections, the IM-2 angle relative to the mantle surface has been reported from 50° to 55° (Ward and Wainwright, 1972; Gosline and Shadwick, 1983; Thompson and Kier, 2001a). However, the exact function of these fibers is less clear.

The IM-3 fibers lie parallel to the circumferential muscle fibers, and are observed to be coiled up while the mantle is in a resting state (Macgillivray et al., 1999). Their orientation suggests that the IM-3 fibers are rarely fully extended while the squid is cruising, but rather aide in the contraction of the mantle after hyperinflation has been used for an especially large jet (Macgillivray et al., 1999).

Problems Addressed

First, the difference between maximizing ejected jet volume and maximizing total volume must be examined. Squid draw propulsive power from a transfer of momentum to a fluid jet. The force acting on the squid during this process is equal to the rate at which the squid transfers momentum to the jet. This force is equal to the product of the jet mass flux and velocity. Both of these quantities are intrinsically related to the muscle contraction rate and the dynamic response of the mantle geometry associated with muscle contraction. Jet velocity and mass flux can be determined from the rate of change of the mantle cavity volume. In this study, we model the muscular contraction as a geometric constraint rather than modeling the complicated dynamics of the muscles themselves. Therefore, the thrust experienced by the squid can be explicitly determined by the structural kinematics of the mantle. The change in mantle cavity volume is modeled with respect to tunic fiber orientation in the subsection Maximizing Jet Volume.

The energy storage capacity of the IM-1 fibers was modeled next. We considered a squid swimming at a steady rate with regular contractions and without hyperinflation. We modeled the squid mantle as a tube circled by inner and outer walls (the tunics) and determined the energy stored by the IM fibers according to the mantle stress–strain dynamics. In developing the energy storage model, it was determined that the elongation of the squid played a crucial role in the energy storage capacity. The fact that the IM-1 collagen fibers lie at a low angle in the sagittal plane causes the strain of individual fibers to have a strong dependence on longitudinal deformation. Although this deformation is small, inclusion in the energy storage model resulted in an optimal fiber orientation in the sagittal plane. This methodology is found in the subsection Maximizing Energy Storage.

METHODS

Maximizing Jet Volume

To analyze the effect of collagen geometry, we constructed a rigid mathematical definition of the fiber orientation. The squid mantle is essentially a tube of interwoven muscle and collagen fibers. The mantle is encased by the tightly woven spiral stacks of the inner and outer tunics. For the purposes of this analysis, each tunic will be modeled as a perfect cylinder composed of helically spiraling fibers (Fig. 1). The parametric equations,

$$\begin{aligned} x &= a\cos(\omega z) \\ y &= a\sin(\omega z) \end{aligned} \quad \text{and} \tag{1}$$

describe the layout of a single tunic fiber, where z is the location of a point along the fiber in the longitudinal direction (starting at the anterior and extending toward the posterior), and x and y are the geometric coordinates of a point on the collagen fiber in the plane normal to the longitudinal axis a distance z from the origin (transverse plane at z). The coordinates in the transverse plane are centered on the longitudinal axis; positive y extends toward the dorsal side, and positive x forms a right handed coordinate system with y and z. The orientation of this coordinate system is depicted in Figure 1. In addition, a is the spiral radius, and ω is a parameter which controls the slope of the spiral (the inverse of ω is the spiral wavelength).

This construct allows us to easily determine several geometric parameters of the cylinder that are necessary to model the mantle mechanics. The cylinder diameter is simply, $D = 2a$, the total cylinder length, L, is the maximum value of the parametric length $L = z_{\max}$, and the tunic fiber angle is defined as $\theta = \arctan(a\omega)$. The length of the tunic fiber is the total arc length of the spiral which is,

$$s = \int_0^L \sqrt{\dot{x}^2 + \dot{y}^2 + 1}\; dz = L\sqrt{a^2\omega^2 + 1}. \tag{2}$$

With these definitions, the cylinder geometry is defined in terms of the tunic fiber angle, θ. This allows the cylinder volume to be calculated as,

$$V = \frac{\pi}{4} D^2 L = \frac{\pi}{4} \left(\frac{s}{2\pi m} \sin\theta \right)^2 s \cos\theta = \frac{s^3}{16\pi m^2} \sin^2\theta \cos\theta \qquad (3)$$

Here, m is the number of spiral windings in the cylinder and s is the fiber length defined in (Eq. 2). It can be seen from (Eq. 3) that the total cylinder volume is purely a function of fiber length, s, and fiber angle, θ. As the collagen fibers are known to have a large low extensibility, we hold the fiber length constant. This imposed constraint reduces the cylinder volume to a function of a single variable, θ. A similar approach has been used to analyze the total squid volume (Vogel, 2003). In the next section of this manuscript, a model is derived describing the energy storage in the collagen fibers which requires deformation of collagen fiber lengths. However, these deformations are very small and can be neglected when defining mantle geometry with minimal error.

It is convenient to clarify our naming convention as there are several characteristic volumes which describe the squid. Equation 3 describes the volume of a cylinder defined by a fiber of length s and angle θ. The total squid volume is the outer tunic's cylindrical volume, V_2. The total internal volume is the inner tunic's cylindrical volume, V_1. The sum of the mantle cavity volume and the internal organs comprises the total internal volume. The difference between the outer tunic cylinder volume and the inner tunic cylinder volume is the mantle volume (or volume of the mantle tissue).

Assuming water to have a constant density, ρ, the mass flux across the funnel will be proportional to the rate of volume change of the inner tunic. Jet velocity can be easily determined from the volume flux if the funnel area, A, is known. This allows the thrust, T, to be described in terms of the tunic geometry to a first-order approximation as:

$$T = \dot{m} u_j = \frac{\rho}{A} \dot{m}^2 = \frac{\rho}{A} \left(\frac{\partial V_1}{\partial t} \right)^2 = \frac{\rho}{A} \left(\frac{\partial V_1}{\partial C_1} \right)^2 \left(\frac{\partial C_1}{\partial t} \right)^2 \qquad (4)$$

Here, $\dot{m}$ is the mass flux across the funnel, u_j is the jet velocity, A is the funnel cross-sectional area, and $C_1 = \pi D_1$ is the circumference of the inner tunic. The rate of change of inner tunic volume, $\partial V_1/\partial t$, is decomposed according to the chain rule into the rate of change of the inner tunic volume with respect to change in the inner tunic circumference, $\partial V_1/\partial C_1$, and the time rate of change of the inner tunic circumference itself, $\partial C_1/\partial t$. As was mentioned previously, the rate at which the circumference contracts is purely defined by the dynamics of the ring muscles and will be treated as a constant. Although the funnel area, A, is known to oscillate with the jetting cycle (Anderson and Demont, 2000; Bartol et al., 2001), for simplicity we will assume that it remains constant. Therefore, the fiber orientation which maximizes $\partial V_1/\partial C_1$ will also maximize the thrust capacity of the squid for any given muscle contraction. It should be noted that maximum $\partial V_1/\partial C_1$ represents the maximum change in the inner tunic cylinder volume, V_1, for a unit differential change in the inner tunic circumference, C_1. This partial derivative is defined here as a function of the inner tunic fiber angle, θ_1, by use of the chain rule:

$$\frac{\partial V_1}{\partial C_1} = \frac{\partial V_1}{\partial \theta_1} \frac{\partial \theta_1}{\partial C_1} \propto \tan\theta_1 \left(3\cos^2\theta_1 - 1\right)$$
$$\text{where} \quad \frac{\partial V_1}{\partial \theta_1} \propto \sin\theta_1 \left(3\cos^2\theta_1 - 1\right) , \qquad (5)$$
$$\text{and} \quad \frac{\partial \theta_1}{\partial C} \propto \frac{1}{\cos\theta_1}$$

where constants have been omitted since we only seek to optimize with respect to θ_1, and are somewhat indifferent to the exact value of $\partial V_1/\partial C_1$ (i.e., the angle which maximizes the volume derivative will be the optimal tunic fiber angle because it results in the largest jet volume for some small contraction of the circumferential muscles, but the actual jet volume for a given contraction is less important).

Maximizing Energy Storage

During slow swimming, the power stroke comes from contracting the circumferential muscles that ring the mantle and contribute the bulk of its mass. The inhalant phase is powered mainly by releasing elastic energy stored during the contraction phase. There is also a set of radial muscles that extend between the inner and outer tunics (Fig. 2); a contraction of these muscles will thin out the mantle layer causing its circumference to re-expand. The IM collagen fibers IM-1 and IM-2 are predicted in some studies to store the necessary mechanical energy with an efficiency approaching 75% (Gosline and Shadwick, 1983). This restoring mechanism allows the mantle composition to heavily favor the circumferential muscles, with a small number of radial muscles accounting for energy losses and providing power for the hyperinflation, required for escape jetting and large amplitude ventilation. This arrangement gives the squid a larger range of jetting capabilities, as such a large portion of the mantle structure is composed of circumferential muscles used actively during jetting.

To model the energy storage process, we investigated the stress–strain dynamics in the mantle structure. We modeled the mantle as a tube defined by an inner and outer helical shell (the inner and outer tunics), whereby the geometry of each shell is defined by Eqs. 1 and 3, and depicted in Figure 1. The mantle geometry can be explicitly defined in terms of shell geometries. The mantle volume is,

$$V_m = \frac{\pi}{4}\left(D_2^2 L_2^2 - D_1^2 L_1^2\right) + \frac{\pi}{6}\left(D_2^2 - D_2 D_1 + D_1^2\right) = f(\theta_1, \theta_2) \qquad (6)$$

Here, D_1, L_1, D_2, L_2 are the diameter and length of the inner and outer tunics, respectively, which can be defined in terms of the inner and outer tunic fiber angles, θ_1 and θ_2, and fiber lengths, s_1 and s_2, as described in the previous section (we assumed that the inner and outer tunic fibers have the same angle at rest $\theta_1 = \theta_2$). Here, again, the tunic fiber lengths are considered to remain constant during the mantle contraction, which means that the tunic fiber angles must change to allow for any change in tunic length and diameter. Therefore, a deformation of the tunic will be modeled by a small shift in the tunic fiber angle, defined as α. It should be noted that a shift in fiber angle will result in coupled changes in volume, length, and diameter. As the jet volume will be equal to the change in internal volume, the shift in inner tunic fiber angle, α_1, can be determined if the jet volume, initial tunic fiber angle, and initial inner tunic volume are known (i.e., $V_j = V(\theta_1 + \alpha_1) - V(\theta_1)$ where V is the volume defined by (Eq. 3) and V_j is the jet volume). Thus, the shift in the inner tunic fiber angle is calculated as the value which achieves the desired jet volume. It should be noted that the actual jet volume, ejected during swimming, has been minimally studied. Most experiments rely on indirect measurements based on wet and dry weights of deceased specimens (Trueman and Packard, 1968; O'Dor and Webber, 1991). The study by Thompson and Kier (2001b) measured the mantle cavity volume more accurately by weighing anesthetized squid with both empty and full mantle cavity. This method should give an appropriate upper bound for the ratio between the jet volume and the total volume, but does not address the possibility that certain swimming behaviors only eject a portion of the fluid in the mantle cavity. This uncertainty will be discussed later in the Results section. Anderson and Demont (2000), approximated the jetting volume during swimming by determining the squid two-dimensional (2D) profile in the sagittal plane and interpolating the total squid volume assuming perfect axial symmetry. However, this approach completely ignores any oblateness or nonuniformity which

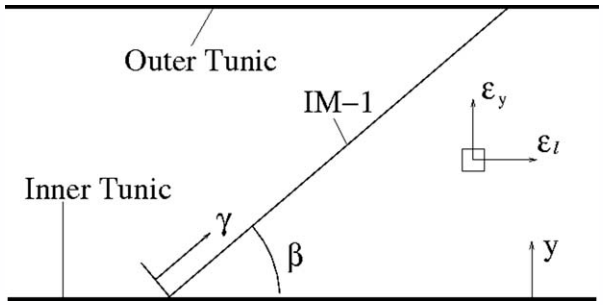

Fig. 3. Strain model construction in the sagittal plane. Here, ϵ is the mantle strain (subscripts indicate direction of strain), y is the radial distance from the inner tunic, γ is the length in the direction of the IM-1 fiber.

might arise during swimming. It has also been qualitatively observed that the paralarvae (early development stages) hold a proportionally greater volume of water in their cavities than juvenile and adult squid (Gilly et al., 1991; Preuss et al., 1997).

To calculate the shift in the outer tunic fiber angle, α_2, we assumed that the mantle volume remained constant during contraction (constant muscle tissue density). The shift in the inner tunic fiber angle is directly correlated to the change in volume required for jetting. This is coupled to a contraction of the diameter and elongation of the length. As a result, the outer tunic must experience a corrective shift in fiber angle which preserves the mantle volume. This shift can be determined by setting the initial mantle volume equal to the final mantle volume,

$$f(\theta_1 + \alpha_1, \theta_2 + \alpha_2) = f(\theta_1, \theta_2), \tag{7}$$

where f is the mantle volume function defined in (Eq. 6). α_2 can now be calculated from (Eq. 7) as θ_1, θ_2, and α_1 are all known. Thus, the geometry of the entire mantle can be determined before and after contraction. The change in geometry will be used to determine the mantle strain characteristics (which will not be uniform).

The energy stored in the mantle structure is directly related to the strain distribution. Similar to a spring system, the energy stored in the collagen fibers is equal to the integral of the stress (force) applied during stretching over the distance (Pilkey and Pilkey, 1974). Furthermore, the stress applied to a material is intrinsically related, by the elastic properties of the material, to the strain (stretching) it experiences. The strain experienced throughout the mantle structure is modeled according to the change in geometry experienced during contraction, and the strain experienced in the fibers themselves is calculated according to their orientation in the mantle. The axial symmetry of the mantle model allows us to define the 3D strain in cylindrical coordinates. In general, the contraction of the mantle's circumferential muscles not only causes the tunic cylinders to decrease in circumference and volume, but also causes the mantle to increase in length and thickness. Thus, the strain in the radial and longitudinal directions will be positive, but the strain in the tangential direction (hoop strain) will be negative during contraction. We analyzed the orientation of the IM-1 fibers in the sagittal plane since this involves the radial and longitudinal components of strain, which are both positive.

Consider a longitudinal slice through the top of the mantle in the sagittal plane. Figure 3 shows the strain orientation and projection of the IM-1 fibers onto this plane. According to the original model construction, the diameter of each tunic is assumed to be constant along its length. This means that the thickness of the mantle will increase uniformly throughout the mantle during contraction. Consequently, the radial component of strain throughout the section will be constant, $\epsilon_y = (h_f - h_0)/h_0$, where $h = (D_2 - D_1)/2$ is the thickness of the mantle, and the subscripts 0 and f refer to the initial and final states of the mantle (before and after contraction), respectively. The lateral strain is slightly more complicated. Both tunics experience a contraction, which results in elongation. However, the amounts by which they contract are not equal ($\alpha_1 \neq \alpha_2$), so their elongations will not be strictly equal either. The lateral strain of each tunic can be determined from the length deformation, $\epsilon_i = \frac{L_{if} - L_{i0}}{L_{i0}}$, where ϵ_i is the tunic strain, and the subscript i can take a value of either 1 or 2 and refers to either the inner or outer tunic, respectively. Assuming that the material on the surface of the tunic experiences the same strain as the tunic itself, and a linear strain distribution, the lateral strain at any location in the section is $\epsilon_l(y) = \epsilon_2 + (\epsilon_1 - \epsilon_2)y/h_f$, where y is the distance from the inner tunic in the radial direction, and h_f is the final mantle thickness. This gives a complete strain distribution in the longitudinal and radial directions, which allows us to define the total strain imposed on a collagen fiber lying in this section.

The stress–strain relationship for collagen fibers is only defined in the direction of the fibers' primary axis, as collagen fibers only support tensile loads, and the energy stored in a given fiber is determined purely by the strain in the direction of that fiber. For a fiber of length b, which is oriented at the IM-1 sagittal angle β with respect to the longitudinal axis, the normal strain can be calculated as,

$$\epsilon_{\text{fiber}} = \frac{1}{b}\int_0^b \left[\epsilon_\ell(y(\gamma))\cos\beta + \epsilon_y \sin\beta\right] d\gamma = \frac{\epsilon_1 + \epsilon_2}{2}\cos\beta + \epsilon_y \sin\beta\,, \tag{8}$$

where γ is a variable which describes position along the length of the fiber (see Fig. 3). Given the final strain in a single fiber as defined by (Eq. 8), the energy stored in that fiber is defined by a simple integral equation

$$E_{\text{fiber}} = \int_0^{\delta_f} F(\epsilon(\delta))\, d\delta = bA_{\text{fiber}} \int_0^{\epsilon_{\text{fiber}}} \sigma(\epsilon)\, d\epsilon \tag{9}$$

In this equation, δ is the change in fiber length, δ_f is the total change after contraction, A_{fiber} is the cross-sectional area of the fiber, F is the stretching force acting on the fiber (tension), and σ is the stress of the fiber which is a function of the strain. Gosline and Shadwick examined the stress–strain relationship for the mantle tissue of *Loligo opalescens* (Gosline and Shadwick, 1983; Fig. 7). A section of the mantle tissue was compressed in the circumferential direction to mimic natural muscle contraction, and the resulting reaction forces were recorded. The mantle tissue was determined to be relatively stiff with an elastic modulus of 2×10^6 Nm^{-2}. Unfortunately, these findings only give the bulk material properties rather than the elastic modulus of the collagen fibers themselves, which is the relationship required for our potential energy model (Eq. 9). To the authors' knowledge, there are no studies which present the elastic properties of individual IM fibers; however, Gosline and Shadwick (1985) performed tensile testing on thin isolated sheets of tunic fibers. As the fibers in the tunic are at very acute angles, this stress–strain relationship should be considered a decent approximation for the stress–strain relationship of individual IM fibers, and has been recreated in Figure 4. These experiments indicated that collagen fibers exhibit a parabolic stress–strain relationship in the low-strain regime ("toe" region), but the slope quickly becomes close to linear and maintains a linear proportionality for the majority of the strain domain. Before reaching the critical breaking stress, there is a very small region where the stress–strain relationship asymptotically plateaus, which is a typical behavior for elastic fibers which deform plastically at high strains, but the transition in collagen is very sharp. Therefore, we modeled the stress–strain relationship as,

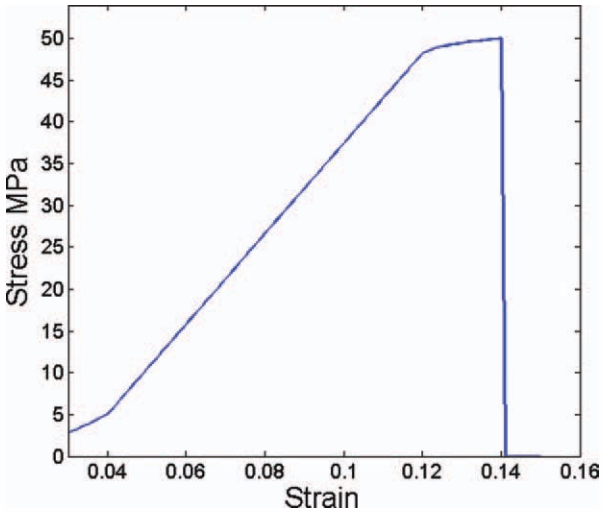

Fig. 4. Stress versus strain relationship used in the model [estimated from Gosline and Shadwick (1985) for a sheet of tunic collagen fibers]. [Color figure can be viewed in the online issue, which is available at wileyonlinelibrary.com.]

$$\sigma = \begin{cases} c_1\epsilon^2 & :\epsilon \le \epsilon_a \\ \sigma_1 + E\epsilon & :\epsilon_a \le \epsilon \le \epsilon_b \\ c_2(\epsilon + c_3)^{1/n} & :\ \epsilon_b \le \epsilon \le \epsilon_m \\ 0 & :\ \epsilon_m < \epsilon \end{cases}, \quad \text{where} \tag{10}$$

$$\begin{matrix} \epsilon_a = 0.04 \\ \epsilon_b = 0.13 \\ \epsilon_m = 0.14 \end{matrix}, \quad \begin{matrix} \sigma_1 = 5\text{MPa} \\ \sigma_1 = 48\text{MPa} \\ \sigma_m = 49\text{MPa} \\ E = 540\text{MPa} \end{matrix}, \quad \begin{matrix} c_1 = \sigma_1/\epsilon_a^2 \\ c_2 = \left(\frac{\sigma_m^2 - \sigma_2^2}{\epsilon_m - \epsilon_b}\right)^{1/n} \\ c_3 = (\sigma_m/c_2) \end{matrix}$$

where ϵ_a, ϵ_b, and ϵ_m are the critical strains in the stress/strain profile corresponding to the beginning and end of the linear region and the critical failure strain, respectively. E is the modulus of elasticity in the linear range (540 MPa), σ_1, σ_2, and σ_m are the stress values corresponding to strains ϵ_a, ϵ_b, and ϵ_m. The values used for all these coefficients were estimated from Gosline and Shadwick (1985, Fig. 5).

This form was chosen because it closely matches the shape of empirical curves obtained for both invertebrate and mammalian collagen (Rigby et al., 1959; Viidik, 1972; Wainright et al., 1976; Gosline and Shadwick, 1983). However, it is hypothesized that the "toe" region is due to the fact that the collagen fibers are still not perfectly aligned with the strain direction, and this is in essence a straightening process. Therefore, the stress–strain relationship was also modeled as a perfect spring with the modulus of elasticity equal to that of the linear region; however, this had very little effect on optimal fiber angles predicted by the model, which is mostly sensitive to the critical stress/strain values, rather than the profile in the low-strain region.

Now all the relationships in the mantle model have been defined so that the total energy stored in a single fiber is found by numerically approximating the integral of Eq. 9, using the stress relationship defined by Eq. 10.

To determine an actual value for total energy storage in the mantle structure several constraints must be imposed. The initial geometry of the mantle was defined according to the length, diameter, and thickness of *S. lessoniana* as were reported in (Thompson and Kier, 2001a). We also assumed that the inner and outer tunics start at the same length which gives a relationship between the fiber lengths of each tunic. The predictions of this model under these constraints will be compared with observed data in the Results section.

RESULTS

Tunic Fiber Orientation

To maximize thrust production, the fiber angle should be aligned so that the ejected volume flux is maximized rather than the total volume. The rate at which fluid is ejected should be considered proportional to the rate of change in the total volume with respect to a change in the circumference, as is derived in Eq. 5.

Figure 5 shows the instantaneous change in tunic cylinder volume with respect to a differential change in circumference, as a function of the initial fiber angle. It can be seen from this figure that, for a small contraction of the circumferential ring muscles, the squid will expel a maximal jet if the initial fiber angle is near 31°. This jet will result in maximum thrust assuming that the ring muscles have a constant rate of contraction (Eq. 4). This angle approaches the actual orientation of tunic fibers measured by Ward and Wainwright (1972).

Intramuscular Fiber Orientation

The squid mantle is oriented so that the circumferential ring muscles (which constitute the bulk of the mantle muscle tissue) provide sufficient compression forces during the jetting phase. However, the refilling phase is driven by sparsely packed radial muscles as well as a release of elastic potential energy stored in the deformed mantle fiber structure.

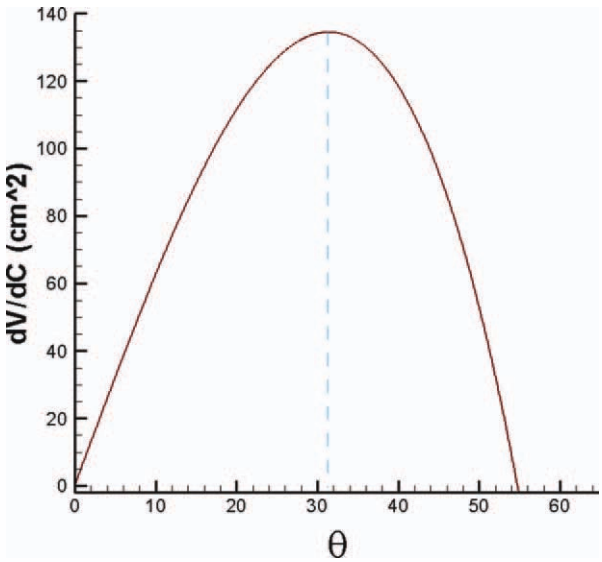

Fig. 5. Differential change in cylinder volume with respect to a contraction of circumference. [Color figure can be viewed in the online issue, which is available at wileyonlinelibrary.com.]

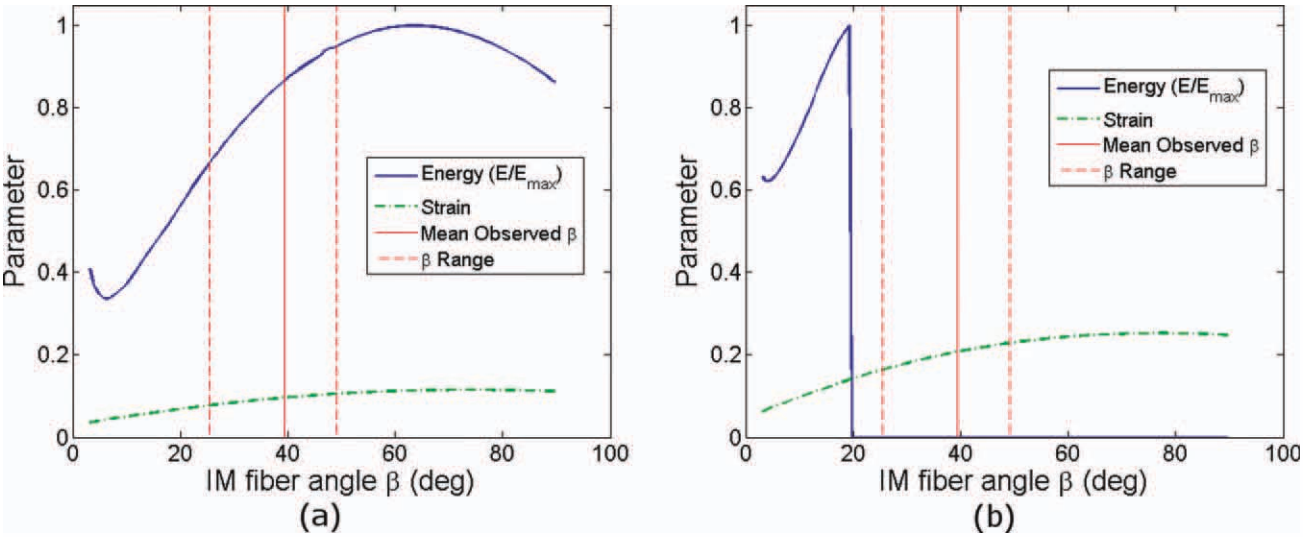

Fig. 6. Energy storage capacity of the mantle structure and IM-1 collagen fiber strain versus fiber angle β. Energy storage capacity as a function of fiber angle is represented by the solid line, fiber strain is shown by the dash-dotted line, and actual distributions of fiber angles are bounded by the vertical band. Energy storage capacity for a cavity volume ratio of 0.25 (**a**) and cavity volume ratio of 0.45 (**b**). [Color figure can be viewed in the online issue, which is available at wileyonlinelibrary.com.]

There is an obvious dichotomy between the tightly packed collagen fibers in the tunics and the scarce IM collagen fibers. The tunic fibers are wound in layers of alternating orientation to form a more or less uniform tube of collagen. The IM fibers, by contrast, are arranged more sparsely throughout the muscle tissue, accounting for 0.1–7% of the total mantle volume, depending on the age of the squid (Thompson and Kier, 2001a). The abundance of collagen fibers in the tunics suggest that these self-reinforced fibers experience minimal stretching compared to the IM fibers. As discussed in the subsection Maximizing Energy Storage, energy is directly related to the deformation of the fibers. The small deformation of tunic fibers results in a low capacity for energy storage, indicating that the tunic fibers primarily serve a structural purpose. In contrast, the high deformation of the IM-1 fibers suggests that they serve as the primary energy storage devices.

Figure 6 shows the normalized energy storage capacity of the IM-1 fibers as a function of the sagittal plane orientation angle β, as was modeled in the subsection Maximizing Energy Storage. The storage capacity was normalized by the maximum achievable energy storage over the β distribution. Figure 6a shows the fiber storage capacity versus β for a jet volume ratio of 0.25, and Figure 6b for a jet volume ratio of 0.45. It can be seen that a squid expelling a jet with a low volume ratio will store a maximum potential energy when the IM-1 fibers are oriented with an angle $\beta = 67^\circ$. The peak in the energy storage capacity curve is very oblate giving a large range of fiber angles with similar energy storage capacity. Conversely, the energy storage capacity for the squid ejecting a jet with a larger volume ratio has a very distinct peak at $\beta = 23^\circ$. This peak does not actually correspond to an equilibrium balance between axial and radial strain, but rather is associated with the failure strain of the collagen fibers; as the fiber angle increases so does the strain in the fiber until the failure strain is reached and the fiber is ruptured.

Data reported for *S. lessoniana* in Thompson and Kier (2001b) was used to define the initial geometry of the mantle (length, diameter, and thickness). This data set was chosen because the mantle geometry and mantle cavity volume ratio, required for the energy storage model, is presented for a large range of squid developmental stages. In addition, the IM fiber angles are given in Thompson and Kier (2001a) corresponding to a similar squid population, providing a reference to validate the model. The values for β over this data set are shown as a vertical band in Figure 6 (bounded on either side by the maximum and minimum observed fiber angles). The cavity volume ratio can vary quite drastically throughout ontogeny, and is more precisely, a maximum bound on the jet volume, and ignores the possibility that during cruising the squid might not eject the entire cavity volume. We used our model to predict optimal fiber angle for the entire range of cavity volume ratios seen in *S. lessoniana* using the mantle geometry associated with that cavity volume ratio, and assuming complete evacuation of the cavity. We also calculated the optimal fiber angle for the same range of jet volume ratios using the mantle geometry of a single adult squid. The optimal fiber angles determined for both ranges of initial conditions are shown in Figure 7. It can be seen that the optimal fiber angles for both conditions are

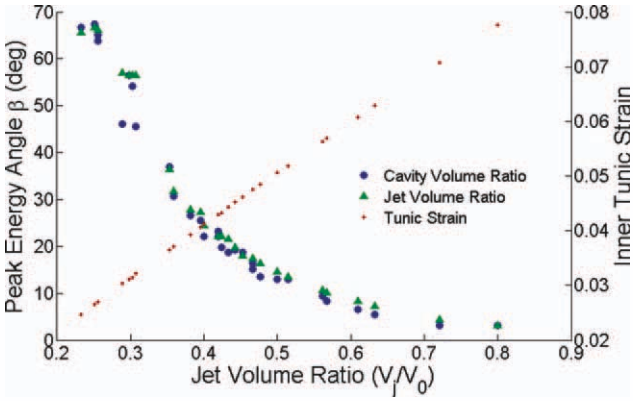

Fig. 7. Optimal IM-1 sagittal fiber angle β as well as inner tunic longitudinal stress ϵ_1 shown as a function of the volume ratio V_j/V. [Color figure can be viewed in the online issue, which is available at wileyonlinelibrary.com.]

nearly identical, indicating that the squid mantle grows such that the relationship between jet volume ratio and mantle strain is preserved.

In addition, the longitudinal strain on the inner tunic was calculated for the same set of volume fractions, and the result is also shown in Figure 7. For the entire range of volume fractions, the longitudinal tunic strain remains very small <8%; a fact which has been observed in previous experiments (Packard and Trueman, 1974). As a result many models have ignored longitudinal tunic strain entirely, thus losing knowledge of a key energy storage mechanism as will be analyzed in the Discussion Section.

The model predicts an optimal fiber angle with respect to jet volume ratio (cavity volume ratio), which can be related to dorsal mantle length (via Thompson and Kier (2001b)). Therefore, we can directly compare the optimal fiber angle predicted by the model with the actual fiber angles observed in the squid (Thompson and Kier, 2001a) over the range of dorsal mantle lengths reported. The large variability in cavity volume fraction for a given dorsal mantle length, results in the model predicting a similarly large range of optimal fiber angles for a given dorsal mantle length. To aid in visualizing this data, the predicted optimal fiber angle was averaged for three mantle length regions (hatchling, juvenile 1 and juvenile 2) which are compared to the actual fiber angle distribution in Figure 8.

DISCUSSION

The use of helically wound high-tensile strength fibers has been examined in the anatomy of several invertebrates with respect to spiral orientation angles. Harris and Crofton (1957) first looked into the effect of the orientation of reinforcing fibers on the length and volume relationship in nematodes. This analysis was extended and applied to both nemerteans and turbellarians (both of which are adept at changing shape) in Clark and Cowey (1958), and determined a relationship between volume and fiber angle for a given length of worm. The volume attains a maximum for a fiber angle near 55°. Similarly, this nominal angle was identified by Harris and Crofton (1957) as the angle that would maintain a constant worm volume for a small deflection in the fiber orientation angle. Vogel (2003) adapted this analysis to squid tunic structures and noted that actual tunic fiber angles will result in a structure that decreases volume with decreased diameter, despite an increase in length, and that the squid volume is maximized at the nominal fiber angle of 55°. However, as is shown in Figure 5, a tunic fiber angle close to 31° will maximize the jet volume flux for a given circumferential muscle contraction (directly related to the jetting thrust), which is very close to actual tunic fiber angles. Figure 5 also shows that when the fiber angle is 55°, there will be no change in volume for a small contraction in circumference (or equivalently diameter), as observed by Harris and Crofton (1957).

Unlike previous studies (Clark and Cowey, 1958; Ward and Wainwright, 1972) which assert that the low angles of the tunic and IM fibers prevent the mantle from changing length, our model incorporates the variation in mantle length during contraction. Our analysis predicts that IM-1 fibers have an optimal angle in the sagittal plane that allows for maximum energy storage. In addition, we find that as length, diameter, and volume are intrinsically coupled, a purely constant mantle length is an overly restrictive assumption and is

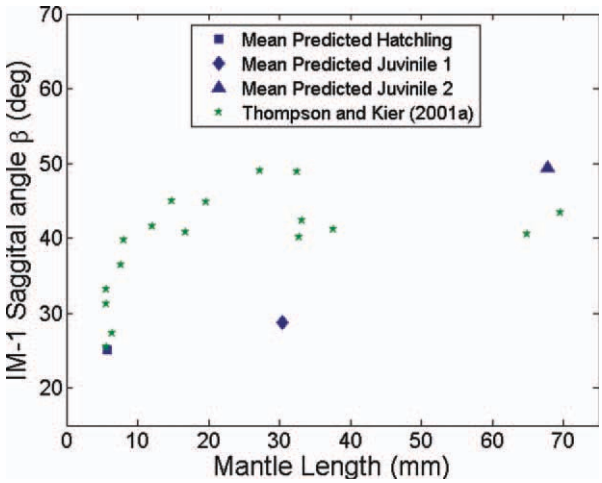

Fig. 8. IM-1 sagittal fiber angle, β, throughout ontogeny. Predicted optimal fiber angles shown by large square, diamond, and triangle markers and actual fiber angles marked by star. [Color figure can be viewed in the online issue, which is available at wileyonlinelibrary.com.]

not required to achieve maximal jet volume. Furthermore, the large aspect ratio of the mantle (being much longer than it is thick), causes a small deformation in length to result in substantial potential energy storage in the longitudinal direction. In fact, the predicted longitudinal strain in the tunics is quite small, 4% in the outer tunic and 4.8% in the inner tunic, which is within the range of longitudinal strains measured by Packard and Trueman (1974). These longitudinal tunic strains were determined assuming a volume ratio of 0.45. In the Results Section, we calculated the longitudinal strain on the inner tunic for several other volume ratios. The sensitivity of tunic strain to volume ratio was shown in Figure 7. It can be seen that even as the jet volume approaches a maximum value of 0.8, the longitudinal tunic strain remains below 8%.

The sensitivity of the optimal IM-1 fiber angle β with respect to cavity volume fraction and jet volume fraction was also shown in Figure 7. The large variation in the optimal fiber angle can be primarily attributed to the fact that large volume ratio contractions produce critical strain in the IM-1 fibers with larger orientation angles in the sagittal plane. In fact, if the fiber is assumed to have a boundless linear stress–strain relationship, the optimal fiber angle varies by only 3°. This means that squid can eject several different size jets with similar mantle energy storage properties. As was previously mentioned, Figure 6a shows that the energy storage capacity has a rather broad peak (when critical strain is not a factor), meaning that there is a large range of fiber angles, β, with favorable energy storage characteristics. Moreover, even the minimum fiber angle observed throughout ontogeny, still has an energy storage capacity close to 70% of predicted maximum for low jet volume ratio. Therefore, the IM-1 fibers are most likely oriented to provide the maximum energy storage, within the limiting physical bounds of the collagen fibers.

The comparison of IM-1 sagittal fiber angles in Figure 8 shows decent agreement between predicted optimal β and actual measured β; but the optimal energy storage model predicts β more acute than that observed, for both hatchling and shorter juvenile squid. First, it should be noted that both of these age groups have the most uncertainty in cavity volume ratio, which will certainly carry over to uncertainty in predicting optimal fiber angles. In addition, the squid mantle is not a perfect cylinder but tapered (like a conical tube), this shape is more pronounced in younger squid, so the cylinder mantle approximation may not be as valid for these young developmental stages.

In the transverse plane, the components of mantle strain were quite different. The radial component of strain (through the thickness) was still defined by the mantle thickness expansion. However, the circumferential component (tangent to the tunic) was negative due to the contraction of the circumferential muscles. As fibers can only store energy under tension (not compression), the IM-2 fibers would store a maximum amount of energy if they were oriented radially (90°). The fact that these fibers are oriented at an angle between 50° and 55° suggests that these fibers are not purely energy storage components, but also serve to transmit forces from the discrete radial muscles to the rest of the mantle.

The various systems of collagen fibers within squid mantle tissue form a complex mechanical system. Several studies have observed a nearly universal orientation of these fiber systems across several species. We have provided a rigid mathematical model to analyze the structural mechanics of the tunic fiber systems, and have determined that the tunic fiber's angle of incidence maximizes the expelled jet volume for a given contraction of circumferential muscles. We have also modeled the energy storage dynamics of the IM-1 fiber system in the sagittal plane. It was shown that the orientation of these fibers maximizes their energy storage capacity, within the physical limitations of the collagen fibers themselves. In addition, it was determined that previous assumptions about the role of IM-1 fibers in restricting longitudinal deformation are not supported by the energy analysis.

ACKNOWLEDGMENTS

The authors thank Connor Fitzhugh for providing several contributions to the article as well as the reviewers who provided substantial corrections and identified studies that measured the required stress/strain relationship for invertebrate collagen fibers.

LITERATURE CITED

Anderson EJ, Demont ME. 2000. The mechanics of locomotion in the squid *Loligo Paelei*: Locomotory function and unsteady hydrodynamics of the jet and intramantle pressure. J Exp Biol 203:2851–2863.

Anderson E, Grosenbaugh M. 2005 Jet flow in steadily swimming adult squid. J Exp Biol 208:1125–1146.

Bartol IK, Patterson MR, Mann R. 2001. Swimming mechanics and behavior of the shallow-water brief squid *Lolliguncula brevis*. J Exp Biol 204:3655–3682.

Bartol IK, Krueger PS, Stewart WJ, Thompson JT. 2008. Swimming dynamics and propulsive efficiency of squids throughout ontogeny. Int Comp Biol 48:720–733.

Bartol IK, Krueger PS, Stewart WJ, Thompson JT. 2009. Hydrodynamics of pulsed jetting in juvenile and adult brief squid *Lolliguncula brevis*: Evidence of multiple jet "modes" and their implications for propulsive efficiency. J Exp Biol 212:1889–1903.

Bone Q, Pulsford A, Chubb AD. 1981. Squid mantle muscle. J Mar Biol Assoc 61:327–342.

Clark RB, Cowey JB. 1958. Factors controlling the change of shape of certain nemertean and turbellarian worms. J Exp Biol 35:731–748.

Dabiri JO, Colin SP, Costello JH. 2006. Fast-swimming hydromedusae exploit velar kinematics to form an optimal vortex wake. J Exp Biol 209:2025–2033.

Gilly WF, Hopkins B, Mackie GO. 1991. Development of giant motor axons and neural control of escape responses in squid embryos and hatchlings. Biol Bull 180:209–220.

Gosline JM, Shadwick RE. 1983. The role of elastic energy storage mechanisms in swimming—an analysis of mantle elasticity in escape jetting in the squid *Loligo opalescens*. Can J Zool 61:1421–1431.

Gosline JM, Shadwick RE. 1985. Molluscan collagen and its mechanical organization in squid mantle (8). In: Hochachka PW, editor. The Molluska, Vol. 1. New York, NY: Academic Press.

Gosline JM, Steeves JD, Harman AD, Demont ME. 1983. Patterns of circular and radial mantle muscle-activity in respiration and jetting of the squid *Loligo opalescens*. J Exp Biol 104:97–109.

Harris JE, Crofton HD. 1957. Structure and function in the nematodes: Internal pressure and cuticular structure in *Ascaris*. J Exp Biol 34:116–130.

Lipinski D, Mohseni K. 2009. A numerical investigation of flow structures and fluid transport with applications to feeding for the hydromedusae *Aequorea victoria* and *Sarsia tubulosa*. J Exp Biol 212:2436–2447.

Macgillivray P, Anderson EJ, Wright GM, DeMont ME. 1999. Structure and mechanics of the squid mantle. J Exp Biol 202:683–695.

O'Dor RK, Webber D. 1991. Invertebrate athletes: Trade-offs between transport efficiency and power density in cephalopod evolution. J Exp Biol 160:93–112.

Packard A, Trueman ER. 1974. Muscular activity of the mantle of *Sepia loligo* (cephalopoda) during respiratory movements and jetting, and its physiological interpretation. J Exp Biol 61:411–419.

Pilkey WD, Pilkey OH. 1974. Stress and strain (4). In: Monti N, editor. Mechanics of Solids. New York: Quantum Publishers. pp 124–129.

Preuss TZ, Lebaric N, Gilly WF. 1997. Post-hatching development of circular mantle muscles in the squid *Loligo opalescens*. Biol Bull 192:375–387.

Rigby BJ, Hirai N, Spikes JD, Eyring H. 1959. The mechanical properties of rat tail tendon. J Gen Physiol 49:265–283.

Sahin M, Mohseni K. 2009. An arbitrary Lagrangian-Eulerian formulation for the numerical simulation of flow patterns generated by the hydromedusa *Aequorea victoria*. J Comp Phys 228:4588–4605.

Sahin M, Mohseni K, Colins S. 2009. The numerical comparison of flow patterns and propulsive performances for the hydromedusae *Sarsia tubulosa* and *Aequorea victoria*. J Exp Biol 212:2656–2667.

Thompson JT, Kier WM. 2001a. Ontogenetic changes in fibrous connective tissue organization in the oval squid, *Sepioteuthis lessoniana* lesson, 1830. Biol Bull 201:136–153.

Thompson JT, Kier WM. 2001b. Ontogenetic changes in mantle kinematics during escape-jet locomotion in the oval squid, *Sepioteuthis lessoniana* Lesson, 1830. Biol Bull 201:154–166.

Trueman ER, Packard A. 1968. Motor performance of some cephalopods. J Exp Biol 49:495–507.

Viidik A. 1972. Simultaneous mechanical and light microscopic studies of collagen fibers. Z Anat 136:204–212.

Vogel S. 2003. Comparative Biomechanics: Life's Physical World. Princeton, NJ: Princeton University Press.

Wainwright SA, Biggs WD, Currey JD, Gosline JM. 1976. Mechanical Design in Organisms. Arnold: London.

Ward DV, Wainwright SA. 1972. Locomotory aspects of squid mantle structure. J Zool 167:437–449.

Young JZ. 1938. The functioning of the giant nerve fibers of the squid. J Exp Biol 15:170–185.